

## PRECISION MEASUREMENTS OF THE NEUTRON SPIN STRUCTURE AT JEFFERSON LAB HALL A

XIAOCHAO ZHENG FOR THE JEFFERSON LAB HALL A AND E97103  
COLLABORATIONS

*Affiliation: Argonne National Lab, Argonne, IL 60439, USA*

*Mailing address: 12000 Jefferson Avenue, Newport News, VA 23606, USA*

*E-mail: xiaochao@jlab.org*

We present here recent progress on the experimental study of the neutron spin structure at Jefferson Lab Hall A. We focus on two precision experiments. The physics motivation and the experimental setup will be described first. Then we present results for the neutron spin asymmetry  $A_1^n$  and results for spin-flavor decomposition of the nucleon spin in the valence quark region, and preliminary results for the neutron spin structure function  $g_2^n$  at low  $Q^2$ .

### 1. Motivation

The structure of the nucleon provides a natural laboratory to study the strong interaction and the theory describing it – quantum chromo-dynamics (QCD). Because the strong interaction has two opposite features, the asymptotic freedom (which can be treated perturbatively) and confinement (which needs a non-perturbative description), it has been the most difficult to study among the four interactions of nature. Deep inelastic scattering (DIS) has served as one of the primary experimental tools to study nucleon structure. DIS data provide information on the behavior of quarks and gluons inside the nucleon, and furthermore how this is governed by the strong interaction. In particular, it has been shown that, at high four momentum transfer square  $Q^2$  and energy transfer  $\nu$ , the process becomes perturbative and can be treated using perturbative QCD (pQCD).

However, although a lot has been learned from data on the unpolarized and polarized structure functions, so far we can only explain their  $Q^2$ -dependence within the framework of QCD, and we are generally unable to make absolute predictions for the structure functions themselves. The virtual photon asymmetry  $A_1$  may provide an exception here: under some assumptions, for the large  $x$  region (where  $x \equiv Q^2/(2M\nu)$  is the Bjorken scaling variable) one can use pQCD to make absolute predictions for the ratio of polarized and unpolarized structure functions,  $g_1/F_1$ , which is approximately  $A_1$  at high  $Q^2$ . The first experiment we present

here is a precision measurement of the neutron  $A_1^n$  in the large  $x$  region. Such data provide crucial information on testing the validity of pQCD and its underlying assumptions in the study of the nucleon spin structure.

Another feature of the strong interaction, as mentioned before, is that it is non-perturbative: the quarks and gluons inside the nucleon cannot be present in nature as free objects (confinement). DIS at low  $Q^2$  may shed light on non-perturbative features of the strong interaction: when  $Q^2$  is small ( $Q^2 < 1 \text{ GeV}^2$ ), the virtual photon tends to see the interaction between the quark it strikes and gluons or other spectator quarks. In the operator product expansion method this is called higher-twist effects. The polarized structure function  $g_2$ , as we will review briefly later, provides a clean tool to study the quark-gluon correlation. The second experiment we present here is a precision measurement of  $g_2$  in the low  $Q^2$  region where the  $q - g$  correlation is expected to be evident. Since the major role played by the gluons inside the nucleon is to bind quarks together, such data will shed light on how confinement arises for the nucleon, which is of great interest in the study of the strong interaction and QCD.

### 1.1. Deep inelastic scattering structure functions

The unpolarized and polarized electromagnetic DIS cross sections are described by the four structure functions:  $F_1(x, Q^2)$ ,  $F_2(x, Q^2)$ ,  $g_1(x, Q^2)$  and  $g_2(x, Q^2)$ . In the simple quark-parton model (QPM),  $F_1$  and  $g_1$  can be related to the unpolarized and polarized parton distribution functions (PDF)  $q_i(x)$  and  $q_i^{\uparrow\downarrow}(x)$ . They describe how the nucleon's momentum is carried by quarks and gluons, and how the quark spins contribute to the nucleon spin. Details of the DIS formulas was summarized in *e.g.* Appendix A of Ref.<sup>1</sup>.

### 1.2. The virtual photon asymmetry $A_1$ at large $x$

The virtual photon asymmetry  $A_1$  measures the cross section difference between scattering with the virtual photon's spin aligned parallel and anti-parallel to the target spin. It can be related to  $g_1$ ,  $g_2$  and  $F_1$  as

$$A_1 = \frac{g_1 - \gamma^2 g_2}{F_1} \quad (1)$$

where  $\gamma^2 = (2Mx)^2/Q^2$ , and  $A_1 \approx g_1/F_1$  at high  $Q^2$ .

The large  $x$  region is of particular interest in the study of nucleon structure. Figure 1 shows the unpolarized PDF from a recent parameterization of world data<sup>2</sup> and the two cartoons illustrate what the nucleon looks like in the small and large  $x$  regions. At small  $x$ , the nucleon can be viewed as being made of a

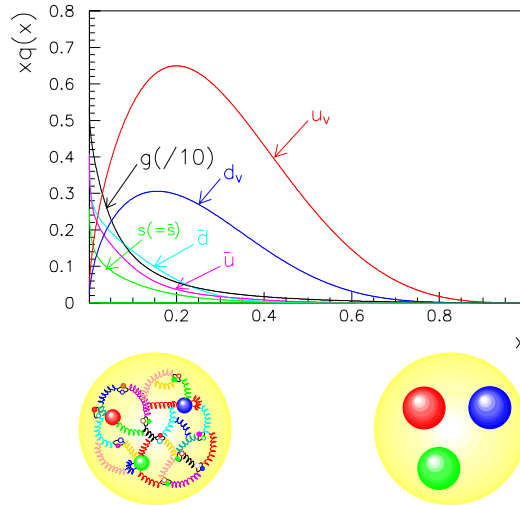


Figure 1. The parton distribution functions from a recent parameterization of world data. The two cartoons illustrated the nucleon structure at small and large  $x$ .

large number of sea quarks and gluons in addition to the three valence quarks. Therefore it is a very complicated many-body system and is difficult to study both experimentally and theoretically. At large  $x$ , the nucleon wavefunction is dominated by the three valence quarks (hence the large  $x$  region is also called the valence quark region) and is easier to model. Because of the same reason, there is less contribution from the sea quarks and gluons to the physics quantities that we observe, so the large  $x$  region is a relatively clean region to study nucleon structure.

There exist many theoretical predictions for the behavior of  $A_1^{p,n}$  in the large  $x$  region. In the relativistic constituent quark model (RCQM),  $A_1^{p,n} \rightarrow 1$  as  $x \rightarrow 1$  because of the hyperfine interaction among the quarks<sup>3</sup>. In pQCD, based on quark helicity conservation and the assumption that the quark transverse motion – hence their orbital angular momentum (OAM) – is negligible in the highly-energetic large  $x$  region, it was predicted that the quark which carries most of the nucleon's momentum should also have the same helicity as the nucleon<sup>4</sup>. This is called hadron helicity conservation (HHC). Based on HHC, one has again  $A_1^{p,n} \rightarrow 1$  as  $x \rightarrow 1$ , although the detailed behavior of how they approach unity is different from the RCQM<sup>5</sup>. Predictions also exist from the LSS parameterization<sup>6</sup>, the statistical model<sup>7</sup> and various other models. Most of the models predict  $A_1^{p,n}$  to be significantly positive in the large  $x$  region. A summary of all predictions can

be found in Refs.<sup>1,8</sup>.

The world data on  $A_1$  for the proton and the neutron, however, have very poor precision in the region  $x > 0.4$ , as can be seen in *e.g.* Figs. 1 and 2 of Ref. <sup>1</sup>. Data on  $A_1^n$  are even consistent with the naive SU(6)-symmetric model prediction  $A_1^n = 0$ . If the data on  $A_1^n$  have turned out to be negative in the large  $x$  region, it would have become a big surprise and it would not be exaggerating to say that another crisis is emerging in the nucleon spin structure study: *Do the CQM (which has been so successful in describing the low energy sector of hadronic physics) and pQCD (which is the perturbative approximation of the most promising theory of the strong interaction) work for the spin structure of the nucleon?* In one word, a precision measurement of  $A_1^n$  in the large  $x$  region is of great importance.

### 1.3. The $g_2$ structure function at low $Q^2$

The structure function  $g_2$ , unlike  $g_1$  and  $F_1$ , cannot be easily interpreted in the simple QPM. To understand  $g_2$  properly, one needs to take into account the transverse motion and the offshell nature of the partons; both arise from the interaction between quarks and gluons, and both cause the QPM to lose its simplicity. In this case, it is easier to study  $g_2$  using the operator product expansion method (OPE) <sup>9</sup>. In the OPE, if neglecting quark masses,  $g_2$  can be cleanly separated into a leading-twist (twist-2) and a higher-twist (twist-3 and higher) term:

$$g_2(x, Q^2) = g_2^{WW}(x, Q^2) + g_2^{H.T.}(x, Q^2). \quad (2)$$

The leading-twist term can be determined from  $g_1$  as <sup>10</sup>

$$g_2^{WW}(x, Q^2) = -g_1(x, Q^2) + \int_x^1 \frac{g_1(y, Q^2)}{y} dy, \quad (3)$$

and the higher-twist term arises from the  $q - g$  ( $t = 3$ ) and  $q - q$  ( $t \geq 4$ ) correlations. Therefore  $g_2$  provides a clean way to study the higher-twist effects. In addition, the  $x^2$ -weighted moment of  $g_2^{H.T.}$  is the twist-3 matrix element <sup>11</sup>:  $d_2 = \int_0^1 x^2 g_2^{H.T.}(x) dx$ . There exist predictions for  $d_2$  from various models and lattice QCD. A summary of predictions can be found in Ref. <sup>12</sup>.

## 2. The $A_1^n$ Experiment – E99117

### 2.1. Overview of the experiment

During experiment E99117 <sup>13</sup> at JLab Hall A, the neutron asymmetry  $A_1^n$  was measured at three  $x$  points in the DIS region, as shown in Table 1. An overall description of the Hall A instrumentation can be found elsewhere <sup>14</sup>. Details of

Table 1. E99-117 kinematics.

	$\langle x \rangle$	0.327	0.466	0.601
$\langle Q^2 \rangle$ (GeV/c) <sup>2</sup>		2.709	3.516	4.833
$\langle W^2 \rangle$ (GeV) <sup>2</sup>		6.462	4.908	4.090

the experiment, the data analysis and all final results have been published previously<sup>1,8</sup>. Here we only briefly describe the experimental setup and the nuclear correction part of the data analysis. We used the JLab polarized electron beam and a polarized  $^3\text{He}$  target in Hall A. A schematic top-view of the hall is given in Fig. 2. The same setup was also used for the experiment to be presented in Section 3. The

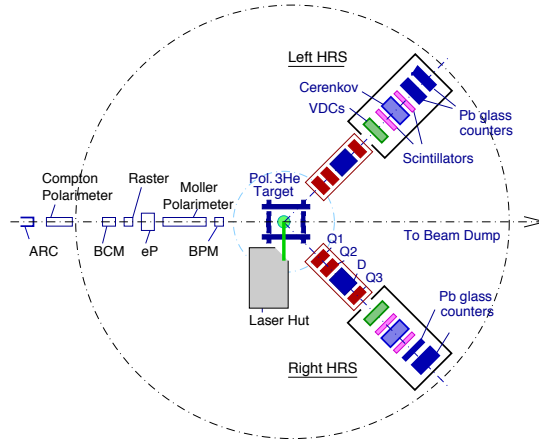


Figure 2. Top-view of experimental setup in JLab Hall A for E99117 and E97103.

beam polarization was measured by Compton and Møller polarimeters<sup>14</sup>. An average value of  $(79.7 \pm 2.4)\%$  was used in the data analysis. The polarized  $^3\text{He}$  target is based on optical pumping and the spin exchange mechanism. The target polarization was measured by two methods: NMR and EPR<sup>1</sup>. The results from two polarimeters were applied in the data analysis on a run-to-run basis. The average value during this experiment was  $P_t = (40.0 \pm 2.4)\%$ .

To extract  $A_1^n$ , we measured both the longitudinal and the transverse asymmetries of the  $\vec{e} - ^3\text{He}$  scattering and calculated  $A_1^{^3\text{He}}$  from the data. Here the polarized  $^3\text{He}$  is used as an effective polarized neutron target because the ground state of  $^3\text{He}$  is dominated by the  $S$  state, in which the two protons' spin anti-align and cancel. This means the spins of the  $^3\text{He}$  nuclei come largely from the neutrons<sup>15</sup>. We took the effective nucleon polarization from various calculations<sup>16</sup>

and used the most recent  $^3\text{He}$  model<sup>17</sup> to extract  $A_1^n$  from  $A_1^{3\text{He}}$ . For the structure functions  $F_2$ ,  $R$ , and  $g_1^p/F_1^p$  needed for this nuclear correction, we used the most up-to-date parameterizations of the world data.

## 2.2. Results for $A_1^n$ and $g_1^n/F_1^n$

Figure 3 shows the results for  $A_1^n$  and  $g_1^n/F_1^n$ , compared with various model predictions and parameterizations. In the region  $x > 0.4$ , the new results have improved the precision of the world data by about an order of magnitude. As for the model predictions, we focus here on only two of them: 1) The prediction from RCQM, although in general higher than the data, gives the correct sign and the  $x \rightarrow 1$  trend. The fact that the difference between the prediction and the data becomes smaller at larger  $x$  is consistent with the expectation that RCQM should work in the valence quark region where the three valence quarks carry most of the nucleon's momentum, spin and quantum numbers and thus can be identified as constituent quarks. 2) The pQCD predictions based on HHC, on the contrary, deviate from data more at larger  $x$  where the perturbative theory is expected to work. This might indicate that there is a problem with the assumption used when deriving the HHC. The first thing to be questioned is the validity of the assumption that the quark OAM is negligible in the  $x$  and  $Q^2$  region explored by this experiment.

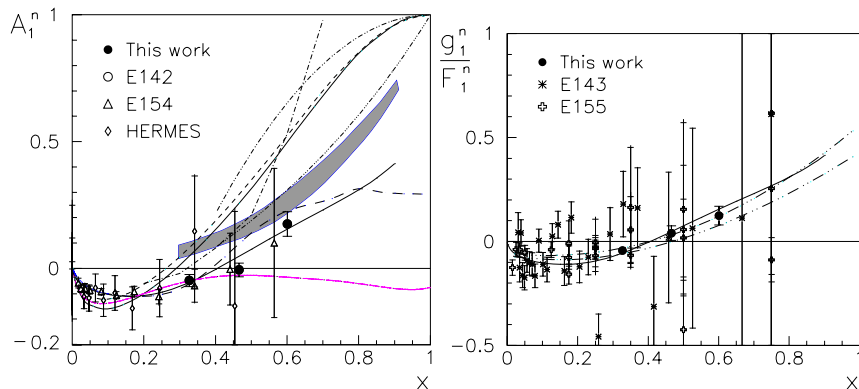


Figure 3. Results on  $A_1^n$  and  $g_1^n/F_1^n$  from E99117. On the left panel, the gray band shows the prediction for  $A_1^n$  from RCQM. The dashed and the higher solid curves (which are very close to each other) are the pQCD HHC-based predictions at  $Q^2 = 4 \text{ (GeV/c)}^2$ , without and with fitting to world data, respectively. See text for curves on the right panel.

A fit of our results and previous world data yields

$$g_1^n/F_1^n = (-0.049 - 0.162 x + 0.698 x^2)(1 + 0.751/Q^2). \quad (4)$$

In Fig. 3 the new fit (dash-dot-dot-dotted) is compared with the LSS2001 parameterization (solid) and the E155 experimental fit (dash-dot-dotted) <sup>18</sup>.

### 2.3. Results for $A_2^n$ and $g_2^n$

Since we have measured both longitudinal and transverse asymmetries, the virtual photon asymmetry  $A_2^n$  and the transverse polarized structure function  $g_2^n$  were also extracted from the data. The results do not show significant deviations from the calculated leading twist contributions. The  $g_2^n$  results at the two high  $x$  points have about half of the uncertainty of previous data from E155x at SLAC <sup>19</sup>. Combined with the E155x data, the twist-3 matrix element for the neutron was extracted as  $d_2^n = 0.0062 \pm 0.0028$ , which also has about half of the uncertainty of the E155x result because of the large- $x$  dominance of the integration.

### 2.4. Flavor decomposition using the simple QPM

In the simple quark-parton model, one can extract polarized PDFs as

$$\frac{\Delta u + \Delta \bar{u}}{u + \bar{u}} = \frac{4g_1^p(4 + R^{du})}{15F_1^p} - \frac{g_1^n(1 + 4R^{du})}{15F_1^n} \quad (5)$$

$$\text{and } \frac{\Delta d + \Delta \bar{d}}{d + \bar{d}} = \frac{4g_1^n(1 + 4R^{du})}{15F_1^n R^{du}} - \frac{g_1^p(4 + R^{du})}{15F_1^p R^{du}}, \quad (6)$$

with  $R^{du} \equiv (d + \bar{d})/(u + \bar{u})$ . We fit to the world proton data  $g_1^p/F_1^p$  and used a recent fit for  $R^{du}$  <sup>20</sup>. The results for  $(\Delta u + \Delta \bar{u})/(u + \bar{u})$  and  $(\Delta d + \Delta \bar{d})/(d + \bar{d})$  extracted from the new  $g_1^n/F_1^n$  data are shown in Fig. 4<sup>a</sup> along with data from semi-inclusive measurements at HERMES <sup>21</sup>. The short-dashed curves are the pQCD HHC-based predictions. For all other curves please see Refs. <sup>1,8</sup>. The figure clearly indicates that there is a problem with the predictions based on HHC. In particular, the quark OAM, or the quark transverse motion, might not be negligible even in the high- $x$  region. To relate these results to the physical picture of the nucleon structure, we use the cartoon on the right panel of Fig. 4: assuming a proton is spinning in a particular direction as shown by the thick (yellow) arrow, when the valence  $u$  quark is hit by the virtual photon, it is seen as spinning in the same direction as the proton spin and having a small OAM (the thin arrowed

<sup>a</sup>The JLab results presented here have been revised, please see Ref<sup>1</sup> for the new values. The results for  $(\Delta d + \Delta \bar{d})/(d + \bar{d})$  changed by about  $1\sigma$  towards the negative side.

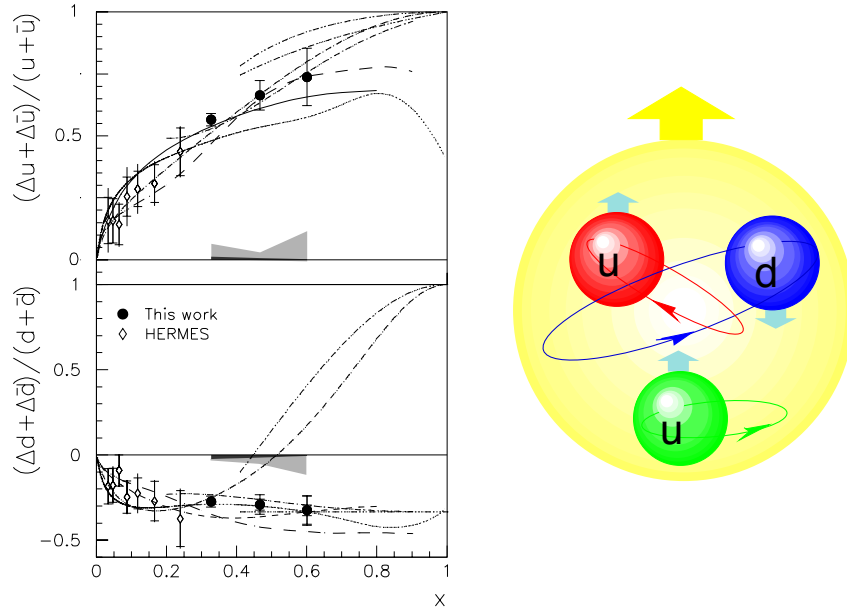


Figure 4. Left panel: results on  $(\Delta u + \Delta \bar{u})/(u + \bar{u})$  and  $(\Delta d + \Delta \bar{d})/(d + \bar{d})$  from experiment E99117. The short-dashed curves are the pQCD HHC-based predictions that  $(\Delta q + \Delta \bar{q})/(q + \bar{q}) \rightarrow 1$  at  $x \rightarrow 1$ . Right panel: a cartoon for the proton spin structure revealed by these results.

ellipse); but when the valence  $d$  quark is hit by the virtual photon, it is found spinning in the opposite direction as the proton spin, but since it possesses a large OAM, the sum of its spin and OAM still gives the proton's overall spin. Obviously, the  $d$  quark behaves very differently from  $u$  quarks inside the proton. This brings a theoretical challenge as the quark OAM and its flavor-dependence has almost never been taken into account properly in all previous large  $x$  calculations.

### 3. E97103 and Preliminary Results on $g_2^n$ at low $Q^2$

During experiment E97103<sup>22</sup> at JLab Hall A, we measured the polarized structure function  $g_2^n$  at five  $Q^2$  points down to  $Q^2 = 0.58$  (GeV/c)<sup>2</sup>. Details of all kinematics are given in Table 2.

Table 2. E97103 kinematics.

$\langle Q^2 \rangle$ (GeV/c) <sup>2</sup>	0.58	0.80	0.96	1.14	1.36
$\langle x \rangle$	0.17	0.18	0.20	0.20	0.21
$\langle W^2 \rangle$ (GeV) <sup>2</sup>	3.82	4.43	4.83	5.57	6.02

The E97103 experiment shared the same instrumentation as the  $A_1^n$  experiment. The main experimental differences between the two were the spectrometer settings, and that more beam time was spent on the transverse target configuration than the longitudinal setting during E97103, while the opposite was true for the  $A_1^n$  measurement. The procedure for data analysis and nuclear corrections of the two experiments is also similar. Details of this experiment and its data analysis can be found in Ref.<sup>23</sup>.

Preliminary results for  $g_2^n$  as well as  $g_1^n$  from E97103 are given in Fig. 5. The light shaded area in the two plots gives the leading-twist contribution to these two quantities, respectively, obtained by fitting to world data and evolving to the  $Q^2$  values of this experiment. The systematic errors are shown as dark shaded area at the horizontal axes. While the new  $g_1^n$  data agree with the leading-twist calculations, a deviation between the new  $g_2^n$  data and its leading-twist contribution can be clearly seen at the three lower  $Q^2$  points, indicating the possible rising of the higher-twist contribution.

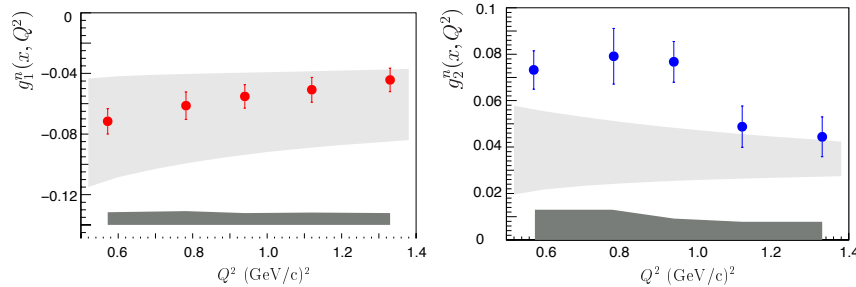


Figure 5. Preliminary results for  $g_1^n$  (left) and  $g_2^n$  (right) from E97103. See text for the meaning of error bands and discussions.

#### 4. Conclusion

We described here recent progress on the neutron spin structure study at Jefferson Lab Hall A. Two experiments and their (preliminary) results were presented. Results for the neutron spin asymmetry  $A_1^n$  at  $x > 0.4$  have a precision about one order of magnitude better than previous world data and the new datum at  $x = 0.61$  is significantly positive, consistent with the prediction from relativistic constituent quark models and various other calculations. These results will serve as crucial inputs to the QCD analysis of parton distribution functions. Results on the flavor decomposition of the nucleon spin  $(\Delta q + \Delta \bar{q})/(q + \bar{q})$  indicate that the quark

orbital angular momentum might play an important role in forming the nucleon spin at large- $x$ , and that the hadron helicity conservation may not hold in the kinematics region explored by this experiment. Preliminary results on the transverse spin structure function of the neutron  $g_2^n$  at  $Q^2 < 1$  (GeV/c)<sup>2</sup> have a precision one order of magnitude better than previous world data. The new results at the three lower  $Q^2$  points below 1 (GeV/c)<sup>2</sup> show a hint of the rising of the higher-twist contribution at low  $Q^2$ .

### Acknowledgments

The author would like to thank the organizing committee for the invitation and their hospitality during the conference. This work is supported in part by the U.S. Department of Energy under Contract No. DE-FC02-94ER40818 and W-31-109-ENG-38. The Southeastern Universities Research Association operates the Thomas Jefferson National Accelerator Facility for the DOE under contract DE-AC05-84ER40150.

### References

1. X. Zheng *et al.*, to appear in Phys. Rev. C.
2. J. Pumplin *et al.*, J. High Energy Phys. **7**, 012 (2002).
3. N. Isgur, Phys. Rev. D **59**, 034013 (1999).
4. G.R. Farrar and D.R. Jackson, Phys. Rev. Lett. **35**, 1416 (1975).
5. S.J. Brodsky, M. Burkardt and I. Schmidt, Nucl. Phys. B **441**, 197 (1995); E. Leader, A.V. Sidorov and D.B. Stamenov, Int. J. Mod. Phys. A **13**, 5573 (1998).
6. E. Leader, A.V. Sidorov and D.B. Stamenov, Eur. Phys. J. C **23**, 479 (2002).
7. C. Bourrely, J. Soffer and F. Buccella, Eur. Phys. J. C **23**, 487 (2002).
8. X. Zheng *et al.*, Phys. Rev. Lett. **92**, 012004 (2004); and various public scientific articles as listed at <http://hallaweb.jlab.org/physics/experiments/he3/A1n/index.html#publications>
9. K. Wilson, Phys. Rev. **179**, 1499 (1969).
10. S. Wandzura and F. Wilczek, Phys. Lett. B **72** (1977).
11. X. Ji and J. Osborne, Nucl. Phys. B **608**, 235 (2001).
12. X. Song, Phys. Rev. D **54**, 1955 (1996).
13. J.-P. Chen, Z.-E. Meziani, P. Souder *et al.*, JLab E99117, <http://hallaweb.jlab.org/physics/experiments/he3/A1n/index.html>
14. J. Alcorn *et al.*, Nucl. Inst. Meth. A **522**, 294 (2004).
15. J.L. Friar *et al.*, Phys. Rev. C **42**, 2310 (1990).
16. A. Nogga, Ph. D. thesis, Ruhr-Universität Bochum, Bochum, Germany (2001), p.72.
17. F. Bissey *et al.*, Phys. Rev. C **65**, 064317 (2002).
18. P.L. Anthony *et al.*, Phys. Lett. B **493**, 19 (2000).
19. P.L. Anthony *et al.*, Phys. Lett. B **553**, 18 (2003).
20. W. Melnitchouk, A. W. Thomas, Phys. Lett. B **377**, 11 (1996).
21. A. Airapetian *et al.*, Phys. Rev. Lett. **92**, 012005 (2004).

22. T. Averett, W. Korsch *et al.*, JLab E97103,  
<http://hallaweb.jlab.org/physics/experiments/he3/g2/temp/>
23. K. Kramer *et al.*, to be submitted to Phys. Rev. Lett.; K. Kramer, Ph.D. thesis, College of William & Mary, 2003.